

Constraints from the decay $B_s^0 \rightarrow \mu^+ \mu^-$ and LHC limits on Supersymmetry

C. Beskidt¹, W. de Boer¹, D.I. Kazakov^{2,3}, F. Ratnikov¹, E. Ziebarth¹, V. Zhukov¹

¹ *Institut für Experimentelle Kernphysik, Karlsruhe Institute of Technology,
P.O. Box 6980, 76128 Karlsruhe, Germany*

² *Bogoliubov Laboratory of Theoretical Physics, Joint Institute for Nuclear Research,
141980, 6 Joliot-Curie, Dubna, Moscow Region, Russia*

³ *Institute for Theoretical and Experimental Physics,
117218, 25 B.Cheremushkinskaya, Moscow, Russia*

Abstract

The pure leptonic decay $B_s^0 \rightarrow \mu^+ \mu^-$ is strongly suppressed in the Standard Model (SM), but can have large enhancements in Supersymmetry, especially at large values of $\tan \beta$. New limits on this decay channel from recent LHC data have been used to claim that these limits restrict the SUSY parameter space even more than the direct searches. However, direct searches are hardly dependent on $\tan \beta$, while $\mathcal{B}r(B_s^0 \rightarrow \mu^+ \mu^-)$ is proportional to $\tan^6 \beta$. The relic density constraint requires large $\tan \beta$ in a large region of the parameter space, which can lead to large values of $B_s^0 \rightarrow \mu^+ \mu^-$. Nevertheless, the experimental upper limit on $\mathcal{B}r(B_s^0 \rightarrow \mu^+ \mu^-)$ is not constraining the parameter space of the CMSSM more than the direct searches and the present Higgs limits, if combined with the relic density. We also observe SUSY parameter regions with negative interferences, where the $B_s^0 \rightarrow \mu^+ \mu^-$ value is up to a factor three below the SM expectation, even at large values of $\tan \beta$.

1 Introduction

Flavour Changing Neutral Currents (FCNC), like the leptonic decays of neutral B-mesons, are strongly suppressed in the Standard Model (SM), since they can only occur via loops involving the weak bosons. These decays are helicity suppressed, so the amplitudes are proportional to the mass of final state particles and the highest rates will be into tau leptons. The experimental signature for leptonic decays is clear: search for an invariant mass in the mass window of the B-meson. This is easier for muonic decays. Hence, muonic B-decays have been investigated in much more detail at hadron colliders, especially since these decays can be strongly enhanced by loop corrections involving particles beyond the SM, like Supersymmetry [1–6]. The $B_s^0 \rightarrow \mu^+ \mu^-$ decay mode has received significant attention [7–9] after the CDF collaboration announced a measurement a factor five to six above the expected SM value [10]. However, the excess was not confirmed by subsequent LHC measurements [11], but

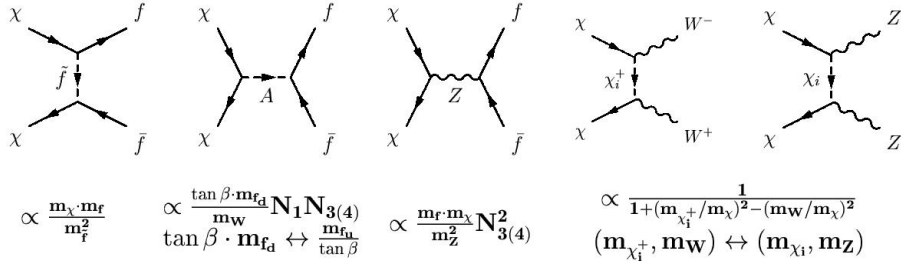


Figure 1: Annihilation diagrams for the lightest neutralino, which is a linear combination of the gaugino and Higgsino states: $|\chi_o\rangle = N_1|B_0\rangle + N_2|W_0^3\rangle + N_3|H_1\rangle + N_4|H_2\rangle$. The dependence of the amplitudes on masses and neutralino mixing parameter N_i has been indicated.

nevertheless the LHC upper limit can give significant constraints on the SUSY parameter space, see e.g. [12], where in some scenarios better limits than those obtained from direct searches have been claimed. However, the excluded parameter space depends strongly on the choice of $\tan \beta$ since the $B_s^0 \rightarrow \mu^+ \mu^-$ rate varies as $\tan^6 \beta$. The relic density constraint correlates $\tan \beta$ with the SUSY mass parameters [13], so if one combines the cosmological constraint with the accelerator constraints there is no arbitrary choice for $\tan \beta$ anymore. Although the relic density requires a large value of $\tan \beta$ in a large region of parameter space, we show that the excluded SUSY mass ranges are well below the LHC constraints from direct searches [14–17] and the limits on the pseudo-scalar Higgs [18, 19]. In principle, other constraints, like $g-2$, $b \rightarrow s \gamma$ and $B \rightarrow \tau \nu$ could also be considered. However taking these into account requires a careful treatment of the non-gaussian systematic errors, which is beyond the scope of the present letter. Numerous studies combining these variables with the recent LHC data have appeared [20–22].

2 Relic Density

The relic density and annihilation cross section σ are related through:

$$\Omega h^2 = \frac{3 \cdot 10^{-27}}{\langle \sigma v \rangle}, \quad (1)$$

where the annihilation cross section σ averaged over the relative velocities of the neutralinos is given in pb [23, 24] and $h \approx 0.71$ is the Hubble constant in units of $100 (km/s)/Mpc$. The best value for the relic density is $\Omega h^2 = 0.1131 \pm 0.0034$ [25]. For a given relic density Ω the annihilation cross section is known independent of a specific model, since it only depends on the observed Hubble constant and the observed relic density. Its value is furthermore largely independent of the neutralino mass m_χ (except for logarithmic corrections)[23, 24]. The DM constraint should exist for any model, but to be specific the Constrained Minimal Supersymmetric Standard Model (CMSSM) with supergravity inspired breaking terms, will be considered [26–28]. It is characterized by 5 parameters: m_0 , $m_{1/2}$, $\tan \beta$, $\text{sign}(\mu)$, A_0 . Here m_0 and $m_{1/2}$ are the common masses for the gauginos and scalars at the GUT scale, which is determined by the unification of the gauge couplings at this scale. Gauge unification is perfectly possible with the latest measured couplings at LEP [29]. Electroweak symmetry breaking (EWSB) fixes the scale of μ [30], so only its sign is a free parameter. The positive sign is taken, as suggested by the small deviation of the SM prediction from the muon anomalous moment.

The relic density can be calculated from the diagrams in Fig. 1. For its calculation we used the public code micrOMEGAs 2.4 [31, 32] combined with Suspect 2.41 as mass spectrum calculator [33]. The optimal parameters were found by minimizing the χ^2 function using the Minuit program [34].

For heavy SUSY masses the sfermion exchange diagram is suppressed, the W- and Z-final states from t-channel chargino and neutralino exchange have a small cross section, the coupling of the LSP to the Z-boson is only via the Higgs component of the LSP, which is typically small, so in most regions of parameter space the pseudo-scalar Higgs exchange is dominant, except for the co-annihilation regions. These are the regions, where the Next-to-Lightest Supersymmetric Particle (NLSP) and LSP are nearly mass-degenerate. In this case they co-exist in the early universe until the common freeze-out temperature and can co-annihilate. This happens if the stau and neutralino are degenerate and co-annihilate into a tau [35]. For this to happen the values of m_0 and $m_{1/2}$ have to be fine-tuned to a high degree, so it happens only in a thin stripe in the $m_0 - m_{1/2}$ plane, as will be shown below. Another co-annihilation region happens at the border of parameter space, where electroweak symmetry breaking does not occur anymore, since here the Higgs mixing parameter becomes negative. In the transition region μ becomes small and the lightest chargino and lightest neutralino become nearly degenerate Higgsinos, as is obvious from the mass matrices, which have as lowest eigenvalues either a gaugino mass term or a Higgsino mass term, if the mixing is neglected. In this case gauginos can co-annihilate into a W-boson [36].

Outside the bulk region with low SUSY masses and the co-annihilation regions the dominant contribution comes from A-boson exchange: $\chi + \chi \rightarrow A \rightarrow b\bar{b}$, which is proportional to

$$\langle \sigma v \rangle \sim \frac{m_\chi^4 m_b^2 \tan^2 \beta (N_{31} \sin \beta - N_{41} \cos \beta)^2 (N_{21} \cos \theta_W - N_{11} \sin \theta_W)^2}{\sin^4 2\theta_W M_Z^2 (4m_\chi^2 - m_A^2)^2 + m_A^2 \Gamma_A^2}. \quad (2)$$

The elements of the mixing matrix in the neutralino sector define the content of the lightest neutralino:

$$|\tilde{\chi}_1^0\rangle = N_{11}|B_0\rangle + N_{21}|W_0^3\rangle + N_{31}|H_1\rangle + N_{41}|H_2\rangle.$$

The sum of the diagrams should yield $\langle \sigma v \rangle = 2 \cdot 10^{-26} \text{ cm}^3/\text{s}$ to get the correct relic density, which implies that the annihilation cross section σ is of the order of a few pb. Such a high cross section can be obtained only close to the resonance, i.e. $m_A \approx 2m_\chi$. Actually on the resonance the cross section is too high, so one needs to be in the tail of the resonance, i.e. $m_A \approx 2.2m_\chi$ or $m_A \approx 1.8m_\chi$. So one expects $m_A \propto m_{1/2}$ from the relic density constraint. This is shown in the left panel of Fig. 2. Here we optimized simply $\tan \beta$ for each pair of $m_0 - m_{1/2}$ values, as was done in Ref. [13]. The corresponding values of $\tan \beta$ needed are shown in the right panel of Fig. 2. The production cross section of the pseudo-scalar Higgs at the LHC is proportional to $\tan^2 \beta$, so the present limits from LHC are proportional to $\tan \beta^2$ as well. At $\tan \beta=50$ the present limit on m_A is about 450 GeV, so the limit on $m_{1/2}$ is close to it. The exclusion on m_A as function of $\tan \beta$ from the CMS collaboration [19] is indicated in Fig. 2 as well. Similar limits have been obtained by the ATLAS collaboration [18]. Also the excluded region from the direct searches has been indicated using the CMS data [16]. Similar results were obtained by other searches [14, 15, 17]. The relic density constraint can be fulfilled with the parameters of Fig. 2, as demonstrated in the left panel of Fig. 3. The top left is excluded, since here the LSP is not a neutral particle, but the stau is the LSP. In the co-annihilation regions the annihilation via the pseudo-scalar Higgs exchange has to be suppressed, thus requiring a larger value of m_A and a corresponding lower value of $\tan \beta$, as demonstrated in the right panel of Fig. 3. It is just a more detailed plot of the right hand panel of Fig. 2 for two values of $m_{1/2}$.

In summary, if one allows $\tan \beta$ to vary in the $m_0 - m_{1/2}$ plane, one obtains the observed relic density for *any* combination of m_0 and $m_{1/2}$, i.e. the relic density allows *all* masses for the SUSY sparticles. However, the $B_s^0 \rightarrow \mu^+ \mu^-$ constraint has to be investigated for the large values of $\tan \beta$ required by the relic density.

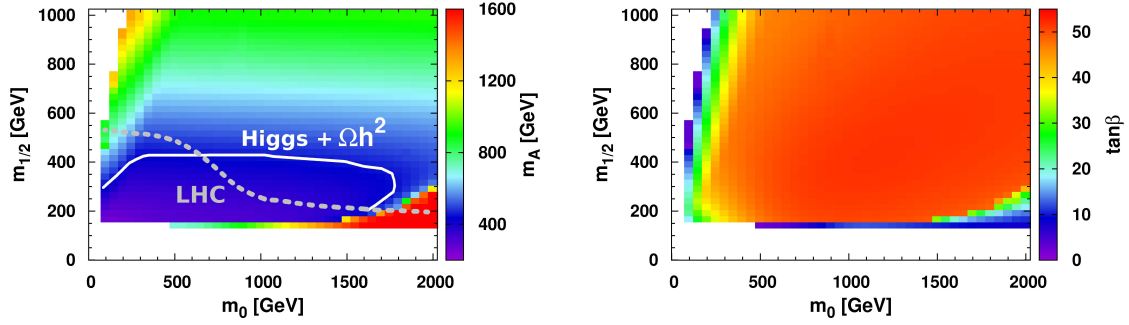


Figure 2: The value of the pseudo-scalar Higgs mass (left) and the value of $\tan\beta$ required for a correct relic density in the $m_0 - m_{1/2}$ plane. The excluded region by the limit on the pseudoscalar Higgs mass from Ref. [19] is indicated by the white solid line in the left panel, while the dashed line indicates the limit from the direct searches from Ref. [16]. The $\tan\beta$ value is around 50 in the central region, as indicated by the colour coding in the right panel and decreases towards the edges, where co-annihilation starts to be important.

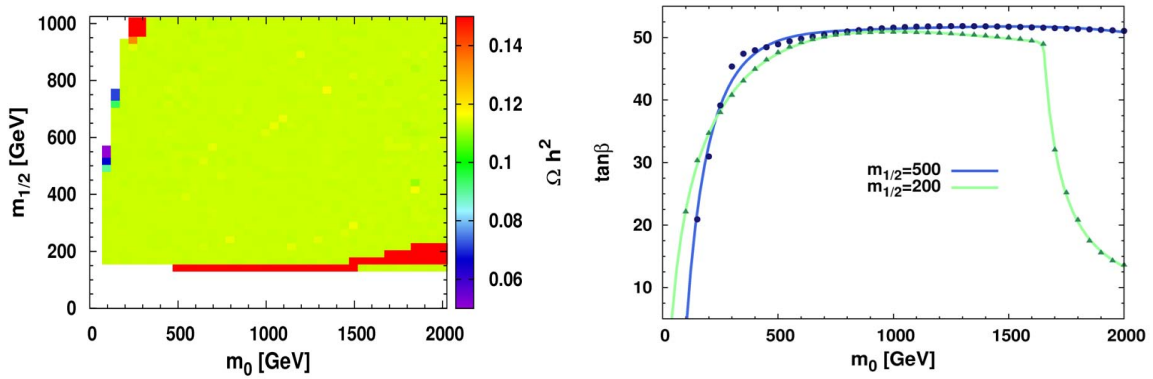


Figure 3: The relic density in the $m_0 - m_{1/2}$ plane (left) and $\tan\beta$ as function m_0 for different values of $m_{1/2}$ (right). The colour coding in the left panel shows that the relic density constraint can be fulfilled for all SUSY masses.

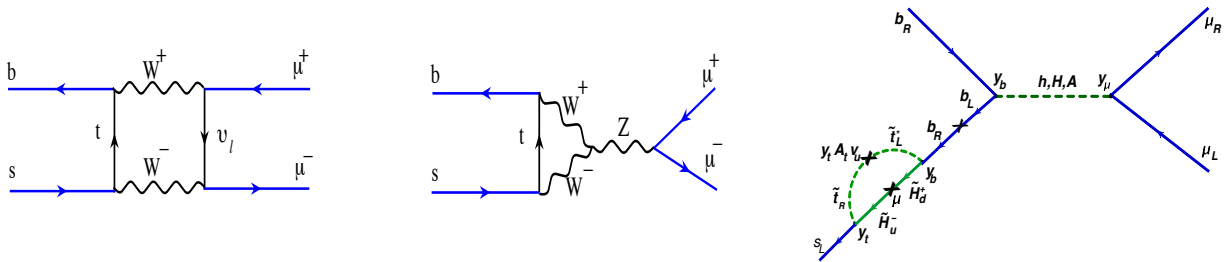


Figure 4: The diagrams contributing to the $B_s^0 \rightarrow \mu^+ \mu^-$ decay in the SM and in the MSSM.

3 $B_s^0 \rightarrow \mu^+ \mu^-$ decay rate

The branching ratio for $B_s^0 \rightarrow \mu^+ \mu^-$ is taken from Ref. [6], which we write in the form

$$\mathcal{B}r(B_s^0 \rightarrow \mu^+ \mu^-) = \frac{2\tau_B m_B^5}{64\pi} f_{B_s}^2 \sqrt{1 - \frac{4m_l^2}{m_B^2}} \left[\left(1 - \frac{4m_l^2}{m_B^2}\right) \left| \frac{(C_S - C'_S)}{(m_b + m_s)} \right|^2 + \left| \frac{(C_P - C'_P)}{(m_b + m_s)} + 2 \frac{m_\mu}{m_{B_s}^2} (C_A - C'_A) \right|^2 \right] \quad (3)$$

where f_{B_s} is the B_s decay constant, m_B is the B meson mass, τ_B is the mean life and m_l is the mass of lepton. C_A, C'_A are largely determined by the SM diagrams, while C_S, C'_S, C_P, C'_P include the SUSY loop contributions due to diagrams involving particles such as stop, chargino, sneutrino, Higgs etc.. For large $\tan\beta$ values the dominant contribution to C_S can be written as:

$$C_S \simeq \frac{G_F \alpha}{\sqrt{2}\pi} V_{tb} V_{ts}^* \left(\frac{\tan^3 \beta}{4 \sin^2 \theta_W} \right) \left(\frac{m_b m_\mu m_t \mu}{M_W^2 M_A^2} \right) \frac{\sin 2\theta_{\tilde{t}}}{2} \left(\frac{m_{\tilde{t}_1}^2 \log \left[\frac{m_{\tilde{t}_1}^2}{\mu^2} \right]}{\mu^2 - m_{\tilde{t}_1}^2} - \frac{m_{\tilde{t}_2}^2 \log \left[\frac{m_{\tilde{t}_2}^2}{\mu^2} \right]}{\mu^2 - m_{\tilde{t}_2}^2} \right) \quad (4)$$

where $m_{\tilde{t}_{1,2}}$ are the two stop masses, and $\theta_{\tilde{t}}$ is the rotation angle to diagonalize the stop mass matrix. We need to multiply the above expression by $1/(1 + \epsilon_b)^2$ to include the SUSY QCD corrections, where ϵ_b is proportional to $\mu \tan\beta$ [37]. We have $C_P = -C_S, C'_S = (m_s/m_b)C_S$ and $C'_P = -(m_s/m_b)C_P$. One observes from Eq. 4 the $\tan^6\beta$ dependence, but one also observes the strong suppression in the last term if the stop masses become equal. In the MSSM the stop mass splitting is given by (see e.g. reviews [38, 39]):

$$\tilde{m}_{1,2}^2 = \frac{1}{2} \left(\tilde{m}_{tL}^2 + \tilde{m}_{tR}^2 \pm \sqrt{(\tilde{m}_{tL}^2 - \tilde{m}_{tR}^2)^2 + 4m_t^2 (A_t - \mu \cot\beta)^2} \right), \quad (5)$$

where the left- and right-handed quark masses are defined by:

$$\begin{aligned} \tilde{m}_{tL}^2 &= \tilde{m}_Q^2 + m_t^2 + \frac{1}{6}(4M_W^2 - M_Z^2) \cos 2\beta, \\ \tilde{m}_{tR}^2 &= \tilde{m}_U^2 + m_t^2 - \frac{2}{3}(M_W^2 - M_Z^2) \cos 2\beta. \end{aligned}$$

For large SUSY scales the mass terms for the right-handed singlet m_U and left-handed doublet m_Q become large and m_{tL} and m_{tR} become of the same order of magnitude. Then the stop splitting is determined by the term $A_t - \mu/\tan\beta$, so for large $\tan\beta$ the second term is small and the stop mixing can be made small by increasing the trilinear coupling A_0 at the GUT scale. One indeed can eliminate the tension between the large value of $\tan\beta$ required by Ωh^2 and the $B_s^0 \rightarrow \mu^+ \mu^-$ rate, as demonstrated in Fig. 5: in the left (right) panel the dependence of $\mathcal{B}r(B_s^0 \rightarrow \mu^+ \mu^-)$ and Ωh^2 are shown as function of $\tan\beta$ for $A_0 = 0$ ($A_0 > 0$). The left and right vertical scales are for $\mathcal{B}r(B_s^0 \rightarrow \mu^+ \mu^-)$ and Ωh^2 , respectively and the scales have been adjusted so, that the horizontal line indicates the upper limit for $\mathcal{B}r(B_s^0 \rightarrow \mu^+ \mu^-)$ and the observed value for Ωh^2 . One observes from the left panel that for the correct value of $\tan\beta=50$ for Ωh^2 the value of $\mathcal{B}r(B_s^0 \rightarrow \mu^+ \mu^-)$ is far above the experimental upper limit, but if one adjusts A_0 both can be brought into agreement (right panel). Here we fitted simply A_0 and $\tan\beta$ for each value of m_0 and $m_{1/2}$ in the $m_0 - m_{1/2}$ plane with $B_s^0 \rightarrow \mu^+ \mu^-$ and Ωh^2 as constraint. The fitted values of A_0 reduce the stop mass to low enough values to force agreement. The required values of A_0 and the corresponding stop mass differences are shown in Fig. 6. The excluded regions in the combined fit of the relic density and $\mathcal{B}r(B_s^0 \rightarrow \mu^+ \mu^-)$ are shown in Fig. 7 for the present limit (left panel) and for a hypothetical limit

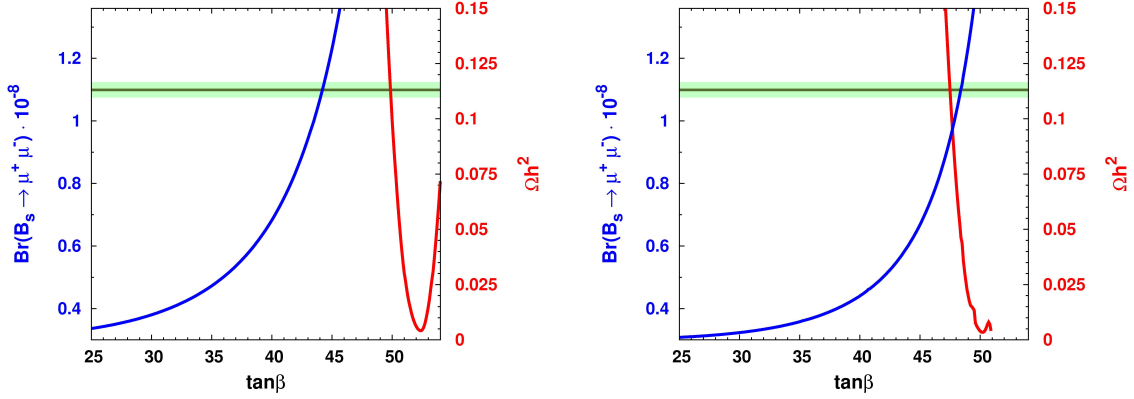


Figure 5: The $\tan\beta$ dependence of $\mathcal{B}r(B_s^0 \rightarrow \mu^+\mu^-)$ and the relic density for $A_0=0$ (left) and $A_0 > 0$ (right). The left and right vertical scales are for $\mathcal{B}r(B_s^0 \rightarrow \mu^+\mu^-)$ and Ωh^2 , respectively and the scales have been adjusted so, that the horizontal line indicates the upper limit for $\mathcal{B}r(B_s^0 \rightarrow \mu^+\mu^-)$ and the observed value for Ωh^2 .

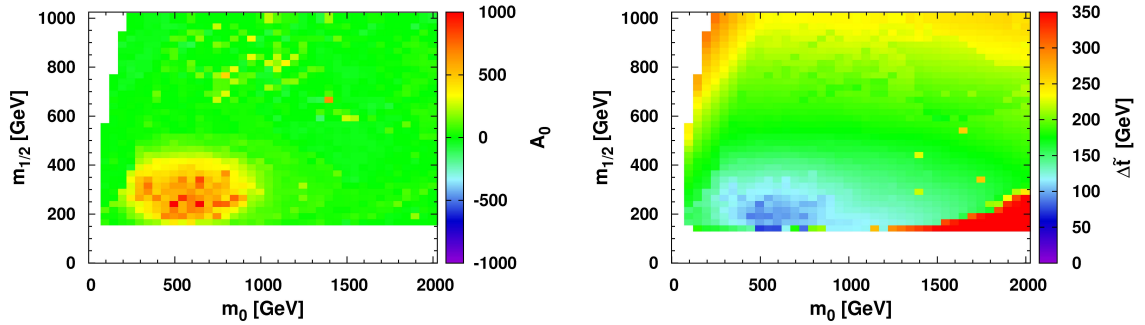


Figure 6: The $\mathcal{B}r(B_s^0 \rightarrow \mu^+\mu^-)$ constraint can lead to tension in combination with the relic density constraint, since the latter requires large $\tan\beta$, which leads to a large stop splitting. However, this can be compensated with a large value of A_0 (left panel), which reduces the difference between the stop masses $\Delta\tilde{t}$ (right panel) in the region where otherwise the constraint $\mathcal{B}r(B_s^0 \rightarrow \mu^+\mu^-) < 4.7 \cdot 10^{-8}$ could not be fulfilled.

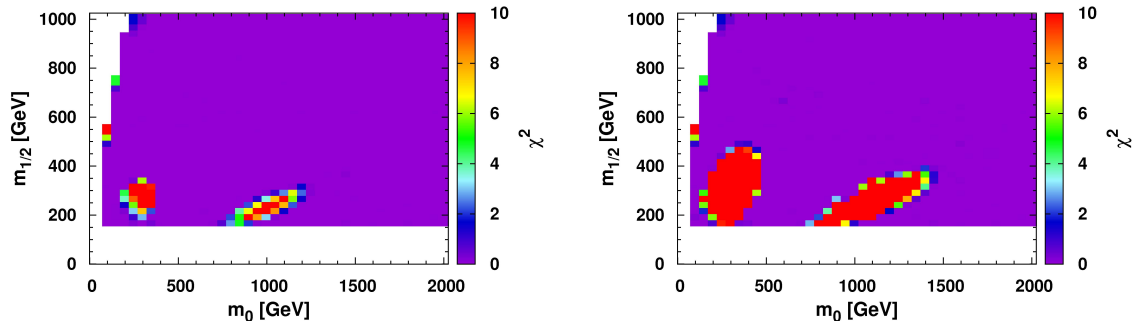


Figure 7: Excluded region from a combined fit of the relic density and the upper limit on $\mathcal{B}r(B_s^0 \rightarrow \mu^+\mu^-) < 1.1 \cdot 10^{-8}$ (left) and a hypothetical $\mathcal{B}r(B_s^0 \rightarrow \mu^+\mu^-) < 0.66 \cdot 10^{-8}$ (right). The colour code indicates the χ^2 value. $\chi^2=5.99$ indicates the 95% C.L. contour, which essentially corresponds to the red region.

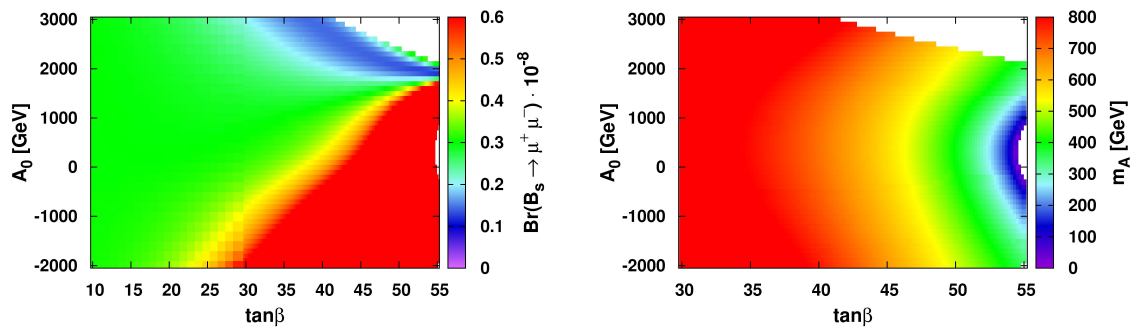


Figure 8: $\mathcal{B}r(B_s^0 \rightarrow \mu^+\mu^-)$ and the pseudoscalar Higgs mass m_A as function of A_0 and $\tan\beta$ in the left and right panel, respectively. The figures corresponds to $m_0 = 1000$ GeV and $m_{1/2} = 250$ GeV, which is inside the excluded region on the right hand side of Fig. 7. Note that the green region in the left panel corresponds to the SM value, while the blue (red) region corresponds to values below (above) the SM value.

of twice the SM value (right panel). One observes that the limit from $\mathcal{B}r(B_s^0 \rightarrow \mu^+\mu^-)$ is well below the limits from the direct and Higgs searches shown in Fig. 2. The reason for the two-lobed excluded regions is the following: at small values of m_0 the trilinear coupling cannot be made large enough to suppress $\mathcal{B}r(B_s^0 \rightarrow \mu^+\mu^-)$ enough, because the staus become tachyonic. At intermediate values of m_0 the trilinear couplings can be made large enough, but at larger values of m_0 the pseudoscalar Higgs boson mass m_A becomes too large for large A_0 values (see Fig. 8 right) and the relic density becomes too large as well. For values of m_0 well above 1 TeV the loop contributions are suppressed enough to fulfill the $\mathcal{B}r(B_s^0 \rightarrow \mu^+\mu^-)$ constraint. These results are demonstrated in Fig. 8, which displays the values of $\mathcal{B}r(B_s^0 \rightarrow \mu^+\mu^-)$ and the pseudoscalar Higgs mass in the A_0 - $\tan\beta$ plane for $m_0 = 1000$ and $m_{1/2} = 250$ GeV, i.e. in the excluded lobe on the right hand side in Fig. 7. The green region in the left pannel of Fig. 8 corresponds to values close to the SM value for $\mathcal{B}r(B_s^0 \rightarrow \mu^+\mu^-)$, but at large positive values of A_0 and large values of $\tan\beta$ the $\mathcal{B}r(B_s^0 \rightarrow \mu^+\mu^-)$ value drops *below* the SM value (blue upper right region), while at lower values of A_0 one observes the famous large $\tan\beta$ enhancement (red bottom right region). In the right top corner the staus become tachyonic, so this theoretically disfavored region is left white. Surprisingly, values of $\mathcal{B}r(B_s^0 \rightarrow \mu^+\mu^-)$ can fall up to a factor three *below* the SM value, which can be explained as follows. In Eq. 4 $\sin(2\theta_{\tilde{t}})$ can change sign, depending on the value of the off-diagonal element in the stop mixing matrix $A_t - \mu/\tan\beta$. Hence, C_P can change sign as well and the term $|(C_P - C'_P)/(m_b + m_s) + 2m_\mu/m_{B_s}^2(C_A - C'_A)|^2$ in Eq. 3 can become small, if C_P and C_A have opposite sign. We have checked that this change in sign is indeed the origin of the negative interference between the SM value and the SUSY values, both in the micrOMEGAs code, which we used, and in the SuperIso V3.1 code [40], which gives almost identical results.

4 Summary

We have calculated the excluded regions in the CMSSM from the recent upper limits on the $B_s^0 \rightarrow \mu^+\mu^-$ decays in combination with the relic density constraint. The latter requires large $\tan\beta$ values in the regions outside the co-annihilation regions and since $\mathcal{B}r(B_s^0 \rightarrow \mu^+\mu^-)$ is proportional to $\tan^6\beta$ one could expect strong constraints from the recent upper limits. However, the $\mathcal{B}r(B_s^0 \rightarrow \mu^+\mu^-)$ approaches zero in case the splitting between the stop1 and stop2 masses approaches zero. This splitting is determined by the off-diagonal element $A_t - \mu/\tan\beta$ of the stop mixing matrix, which can be made small for large $\tan\beta$ and a positive value of the trilinear coupling A_0 at the GUT scale. From a simultaneous fit of A_0 and $\tan\beta$ to the combined data of $\mathcal{B}r(B_s^0 \rightarrow \mu^+\mu^-)$ and relic density we find the excluded regions from these constraints to be well below the constraints from the Higgs searches and direct searches at the LHC. This holds even in the case that a hypothetical limit on $\mathcal{B}r(B_s^0 \rightarrow \mu^+\mu^-)$ of two times the SM value would be obtained.

It is also shown that at large values of both, $\tan\beta$ and the trilinear coupling, negative interferences can lead to $\mathcal{B}r(B_s^0 \rightarrow \mu^+\mu^-)$ values a factor three below the SM value, so even if values below the SM are found experimentally, this does not exclude supersymmetry, but constrains the parameter space.

5 Acknowledgements

Support from the Deutsche Forschungsgemeinschaft (DFG) via a Mercator Professorship (Prof. Kazakov) and the Graduiertenkolleg "Hochenergiephysik und Teilchenastrophysik" in Karlsruhe is greatly appreciated. Furthermore, support from the Deutsche Luft und Raumfahrt (DLR) and the Bundesministerium for Bildung und Forschung (BMBF) is acknowledged.

References

- [1] C.-S. Huang, W. Liao, and Q.-S. Yan, “The Promising process to distinguish supersymmetric models with large tan Beta from the standard model: $B_s \rightarrow \mu^+ \mu^-$ ”, *Phys.Rev.* **D59** (1999) 011701, [arXiv:hep-ph/9803460](#).
- [2] S. R. Choudhury and N. Gaur, “Dileptonic decay of B/s meson in SUSY models with large tan(beta)”, *Phys. Lett.* **B451** (1999) 86–92, [arXiv:hep-ph/9810307](#).
- [3] K. S. Babu and C. F. Kolda, “Higgs mediated $B_s \rightarrow \mu^+ \mu^-$ in minimal supersymmetry”, *Phys. Rev. Lett.* **84** (2000) 228–231, [arXiv:hep-ph/9909476](#).
- [4] A. Dedes, H. K. Dreiner, and U. Nierste, “Correlation of $B_s \rightarrow \mu^+ \mu^-$ and (g-2) (μ) in minimal supergravity”, *Phys.Rev.Lett.* **87** (2001) 251804, [arXiv:hep-ph/0108037](#).
- [5] C. Bobeth, T. Ewerth, F. Kruger et al., “Enhancement of $B(\text{anti-}B(d) \rightarrow \mu^+ \mu^-) / B(\text{anti-}B(s) \rightarrow \mu^+ \mu^-)$ in the MSSM with minimal flavor violation and large tan beta”, *Phys.Rev.* **D66** (2002) 074021, [arXiv:hep-ph/0204225](#).
- [6] R. L. Arnowitt, B. Dutta, T. Kamon et al., “Detection of $B_s \rightarrow \mu^+ \mu^-$ at the Tevatron run II and constraints on the SUSY parameter space”, *Phys. Lett.* **B538** (2002) 121–129, [arXiv:hep-ph/0203069](#).
- [7] B. Dutta, Y. Mimura, and Y. Santoso, “ $B_s \rightarrow \mu^+ \mu^-$ in Supersymmetric Grand Unified Theories”, [arXiv:1107.3020](#).
- [8] P. N. S. Akula, D. Feldman and G. Peim, “Excess Observed in CDF $B_s^0 \rightarrow \mu^+ \mu^-$ and SUSY at the LHC”, [arXiv:1107.3535](#).
- [9] D. Hooper and C. Kelso, “Implications of a Large $B_s \rightarrow \mu^+ \mu^-$ Branching Fraction for the Minimal Supersymmetric Standard Model”, [arXiv:1107.3858](#).
- [10] CDF Collaboration, “Search for $B_s \rightarrow \mu^+ \mu^-$ and $B_d \rightarrow \mu^+ \mu^-$ Decays with CDF II”, [arXiv:1107.2304](#).
- [11] CMS, LHCb, and Coll., “Search for the rare decay $B_s^0 \rightarrow \mu^+ \mu^-$ at the LHC”, **LHCb-CONF-2011-047, CMS PAS BPH-11-019** (2011).
- [12] A. G. Akeroyd, F. Mahmoudi, and D. M. Santos, “The decay $B_s^0 \rightarrow \mu^+ \mu^-$: updated SUSY constraints and prospects”, [arXiv:1108.3018](#).
- [13] C. Beskidt et al., “Constraints on Supersymmetry from Relic Density compared with future Higgs Searches at the LHC”, *Phys. Lett.* **B695** (2011) 143–148, [arXiv:1008.2150](#).
- [14] ATLAS Collaboration, “Search for supersymmetric particles in events with lepton pairs and large missing transverse momentum in 7 TeV proton-proton collisions with the ATLAS experiment”, [arXiv:1103.6214](#).
- [15] ATLAS Collaboration, “Search for supersymmetry using final states with one lepton, jets, and missing transverse momentum with the ATLAS detector at 7 TeV”, *Phys.Rev.Lett.* **106** (2011) 131802, [arXiv:1102.2357](#).
- [16] CMS Collaboration, “Search for Supersymmetry at the LHC in Events with Jets and Missing Transverse Energy”, [arXiv:1109.2352](#).

- [17] CMS Collaboration, “Search for supersymmetry in pp collisions at 7 TeV in events with a single lepton, jets, and missing transverse momentum”, [arXiv:1107.1870](#).
- [18] ATLAS Collaboration, “Search for neutral MSSM Higgs bosons decaying to tau tau pairs in proton-proton collisions at 7 TeV with the ATLAS detector”, [arXiv:1107.5003](#).
- [19] CMS. Collaboration, “Search for Neutral Higgs Bosons Decaying to Tau Pairs in pp Collisions at $\sqrt{s}=7$ TeV”, **CMS-PAS-HIG-11-009** (2011).
- [20] O. Buchmueller, R. Cavanaugh, D. Colling, A. De Roeck, M. J. Dolan, J. R. Ellis, H. Flacher, S. Heinemeyer *et al.*, “Supersymmetry and Dark Matter in Light of LHC 2010 and Xenon100 Data,” *Eur. Phys. J.* **C71**, 1722 (2011). [arXiv:1106.2529](#).
- [21] G. Bertone, D. G. Cerdeno, M. Fornasa, R. R. de Austri, C. Strece, R. Trotta, “Global fits of the cMSSM including the first LHC and XENON100 data,” [arXiv:1107.1715](#).
- [22] S. Sekmen, S. Kraml, J. Lykken, F. Moortgat, S. Padhi, L. Pape, M. Pierini, H. B. Prosper *et al.*, “Interpreting LHC SUSY searches in the phenomenological MSSM,” [arXiv:1109.5119](#).
- [23] E. W. Kolb and M. S. Turner, “The Early universe”, *Front.Phys.* **69** (1990) 1–547.
- [24] G. Jungman, M. Kamionkowski, and K. Griest, “Supersymmetric dark matter”, *Phys.Rept.* **267** (1996) 195–373, [arXiv:hep-ph/9506380](#).
- [25] WMAP Collaboration, “Seven-Year Wilkinson Microwave Anisotropy Probe (WMAP) Observations: Cosmological Interpretation”, *Astrophys.J.Suppl.* **192** (2011) 18, [arXiv:1001.4538](#).
- [26] A. R. L. Chamseddine, A. H. and P. Nath, “Masses of Superpartners of Quarks, Leptons, and Gauge Mesons in Supergravity Grand Unified Theories”, *Phys.Rev.Lett.* **49** (1982) 970.
- [27] P. Nath, R. L. Arnowitt, and A. H. Chamseddine *Nucl. Phys.* **B227** (1983) 121.
- [28] L. J. Hall, J. D. Lykken, and S. Weinberg, “Supergravity as the Messenger of Supersymmetry Breaking”, *Phys.Rev.* **D27** (1983) 2359–2378.
- [29] W. de Boer and C. Sander, “Global electroweak fits and gauge coupling unification”, *Phys.Lett.* **B585** (2004) 276–286, [arXiv:hep-ph/0307049](#).
- [30] K. Inoue, A. Kakuto, H. Komatsu *et al.*, “Aspects of Grand Unified Models with Softly Broken Supersymmetry”, *Prog.Theor.Phys.* **68** (1982) 927.
- [31] G. Belanger, F. Boudjema, A. Pukhov *et al.*, “micrOMEGAs: A Tool for dark matter studies”, [arXiv:1005.4133](#).
- [32] A. Pukhov, G. Belanger, F. Boudjema *et al.*, “Tools for Dark Matter in Particle and Astroparticle Physics”, *PoS ACAT2010* (2010) 011, [arXiv:1007.5023](#).
- [33] A. Djouadi, J.-L. Kneur, and G. Moultaka, “SuSpect: A Fortran code for the supersymmetric and Higgs particle spectrum in the MSSM”, *Comput.Phys.Commun.* **176** (2007) 426–455, [arXiv:hep-ph/0211331](#).
- [34] F. James and M. Roos, “Minuit: A System for Function Minimization and Analysis of the Parameter Errors and Correlations”, *Comput.Phys.Commun.* **10** (1975) 343–367.

- [35] J. R. Ellis, T. Falk, K. A. Olive et al., “Calculations of neutralino-stau coannihilation channels and the cosmologically relevant region of MSSM parameter space”, *Astropart.Phys.* **13** (2000) 181–213, [arXiv:hep-ph/9905481](#).
- [36] K. Griest and D. Seckel, “Three exceptions in the calculation of relic abundances”, *Phys.Rev.* **D43** (1991) 3191–3203.
- [37] M. S. Carena, D. Garcia, U. Nierste et al., “Effective Lagrangian for the $\bar{t}bH^+$ interaction in the MSSM and charged Higgs phenomenology”, *Nucl.Phys.* **B577** (2000) 88–120, [arXiv:hep-ph/9912516](#).
- [38] W. de Boer, “Grand unified theories and supersymmetry in particle physics and cosmology”, *Prog.Part.Nucl.Phys.* **33** (1994) 201–302, [arXiv:hep-ph/9402266](#).
- [39] D. Kazakov, “Supersymmetry on the Run: LHC and Dark Matter”, *Nucl.Phys.Proc.Suppl.* **203-204** (2010) 118–154, [arXiv:1010.5419](#).
- [40] A. Arbey and F. Mahmoudi, “SuperIso Relic: A Program for calculating relic density and flavor physics observables in Supersymmetry”, *Comput.Phys.Commun.* **181** (2010) 1277–1292, [arXiv:0906.0369](#).